Heliyon 9 (2023) e23116

Contents lists available at ScienceDirect

Heliyon

journal homepage: www.cell.com/heliyon

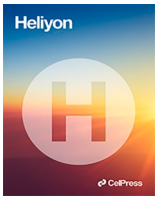

Toxicity study of rats treated by plasma-activated solution

Fanfan Chen [a,1], Houyu He [a,1], Liyun Wang [a], Xingyu Yang [a], Jing Gao [a], Jingwen Wang [a], Shengquan Zhang [b,c], Shenghai Huang [d], Chunjun Yang [a,*]

[a] Department of Dermatology, The Second Affiliated Hospital, Anhui Medical University, Hefei, 230601, Anhui, PR China
[b] Anhui Provincial Institute of Translational Medicine, Hefei, 230032, Anhui, PR China
[c] Department of Biochemistry and Molecular Biology, School of Basic Medical Sciences, Anhui Medical University, Hefei, 230032, Anhui, PR China
[d] Department of Microbiology, Anhui Medical University, Hefei, 230032, Anhui, PR China

ARTICLE INFO

Keywords:
Cold atmospheric plasma
Plasma-activated solution
Safety study
Immunohistochemistry
Angiogenesis

ABSTRACT

Background: Cold atmospheric plasma (CAP) is an effective treatment for various skin diseases. Plasma-activated solution (PAS) is an indirect method of CAP treatment that produces biological effects similar to those of direct treatment with plasma devices. The anticancer and bacteriostatic effects of PAS have been demonstrated in vitro experiments; however, on the basis of the lack of toxicological studies on PAS, its effects on living mammals when administered by subcutaneous injection is poorly known.

Purpose: The purpose of this study was to evaluate the effects of PAS on local skin tissue cells, blood system, heart, liver, lungs, kidneys and other vital organs of the rat when injected subcutaneously.

Methods: PAS was prepared by CAP irradiation of phosphate-buffered saline (PBS). PBS and different PBS groups (CAP irradiation for 1, 3, or 5 min) were injected subcutaneously once every 48 h. The rats were euthanized immediately after 10 cycles of therapy.

Results: No adverse effects were observed during the entire period of the experiment. Histopathological examination of organs and tissues revealed no structural changes. Moreover, no obvious structural changes were observed in skin tissue. DNA damage and cancerous proliferative changes were not detected in skin tissue treated with PAS. Subsequently, RNA sequencing and western blotting were performed. The results showed that PAS increased the expression of growth factors like transforming growth factor beta (TGF-β) and vascular endothelial growth factor A (VEGFA). These results might be directly linked to the role of PAS in stimulating TGF-β receptor signaling pathway and angiogenesis.

Abbreviations: ALT, Glutamic pyruvic transaminase; AST, Glutamic oxaloacetic transaminase; BAS, Basophils; BPs, Biological processes; BSA, Bovine serum; BUN, Blood urea nitrogen; CAP, Cold atmospheric plasma; CCs, Cell components; CREAT, Creatinine; DEG, Differentially expressed gene; EOS, Eosinophils; GAPDH, Glyceraldehyde-3-phosphate dehydrogenase; HGB, Hemoglobin; H2O2, Hydrogen peroxide; LYM, Lymphocytes; MCH, Mean corpuscular hemoglobin; MCV, Mean corpuscular volume; MDA, Malondialdehyde; MFs, Molecular functions; MON, Monocytes; NEU, Neutrophils; PAS, Plasma-Activated Solution; PBS, Phosphate buffer saline; PLT, Platelets; PVDF, Polyvinylidene Fluoride; RBC, Red blood cells; RDWc, Red cell distribution width; RNS, Nitrogen reactive species; ROS, Oxygen reactive species; SDS-PAGE, Sodium dodecyl sulfate polyacrylamide; SOD, Superoxide Dismutase; TGFβ, Transforming growth factor beta; TNFα, Tumor necrosis factor alpha; VEGFA, Vascular endothelial growth factor A; WBC, White blood cells; γ-H2AX, Phosphorylated histone H2AX.

* Corresponding author.
E-mail addresses: 879181414@qq.com (F. Chen), 1103215013@qq.com (H. He), 1961141083@qq.com (L. Wang), 1254212653@qq.com (X. Yang), gaojing0510@126.com (J. Gao), wangjingwen1988@163.com (J. Wang), shengquanzhang1@sina.com (S. Zhang), shenghaihuang1@gmail.com (S. Huang), yangchunjun9@163.com (C. Yang).
[1] These authors contributed equally to this work.

https://doi.org/10.1016/j.heliyon.2023.e23116
Received 11 May 2023; Received in revised form 26 November 2023; Accepted 27 November 2023
Available online 2 December 2023

Conclusion: The results showed that multiple subcutaneous injections of PAS did not show significant toxic side effects on local skin tissues and some vital organs in rats, providing a scientific basis to support the future treatment of skin diseases with PAS.

1. Introduction

Cold atmospheric plasma (CAP) can be produced at mild temperatures and atmospheric pressure and can directly interact with tissues and cells without causing thermal damage. Thus, it has received widespread attention in the biomedical field [1]. CAP contains electromagnetic radiation, including electric, ultraviolet (UV), free electrons, free radicals, oxygen reactive species (ROS), and nitrogen reactive species (RNS) (e.g., H2O2, OH, O3, NO, NO2, etc.) [2–5]. It has exhibited beneficial effects in sterilization [6], promoting wound healing [7], pro-coagulation [8], cancer treatment [9,10], skin disease treatment and cosmetic dermatology [11–13].

The cold atmospheric plasma-activated solution (PAS) is an ROS/RON-wealthy "activation solution" prepared by CAP discharge treatment for pure water, physiological saline, cell culture medium, and other liquids, and is an indirect way for CAP treatment [14]. The PAS treatment of cells or tissues can produce biological effects similar to those of direct treatment with plasma devices [15]. In some cases, direct CAP treatment fails to reach the deeper tissues. Therefore, considering the limitations of equipment and storage, PAS has received considerable attention in recent years.

CAP, a convenient and widely used treatment, has been shown to have beneficial effects on superficial skin trauma, tumors, and inflammatory skin diseases (e.g., specific dermatitis) [3]. It is worth noting that an enhanced uptake rate was achieved when the chemical or drug was added with direct and indirect plasma treatments [16,17]. Direct treatment is simple, convenient, and reach tissues inaccessible through direct irradiation. Therefore, intradermal injection of PAS alone or in combination with chemotherapeutic drugs is a wise choice for the skin tissue infections and benign and malignant tumors of the skin (e.g., hemangioma, basal cell carcinoma, and squamous cell carcinoma).

The mechanisms of CAP-cell interactions are complex. Recent research suggests that CAP induces oxidative stress in cellular tissues by producing ROS/RON [18,19]. However, excess exogenous ROS/RON may break the oxidative equilibrium of the cellular microenvironment, thereby resulting in a series of cytotoxic reactions [20,21]. In the future, PAS may be used to treat benign and malignant tumors of the skin and skin tissue infections [3]. In such cases, especially when injected subcutaneously, it may be in direct contact with normal skin keratinocytes, fibroblasts, and vascular endothelial cells, thereby affecting healthy skin tissue and human health. However, there is no clear definition of plasma dose so far. Different plasma treatment doses are responsible for different cellular effects. In this study, we defined the plasma treatment time as the dose [22]. To date, the effects produced by subcutaneous injections of PAS in live mammals have not been evaluated. The question, therefore, 'Does subcutaneous injection of PAS negatively affect local and some vital organs?' remains unanswered. Based on this issue, this study was conducted to evaluate the effect of subcutaneous injection of PAS on normal skin tissues and some vital organs in rats.

2. Materials and methods

2.1. Preparation of PAS

The atmospheric-pressure plasma source used to prepare the PAS was dielectric barrier discharge (DBD), which was designed and

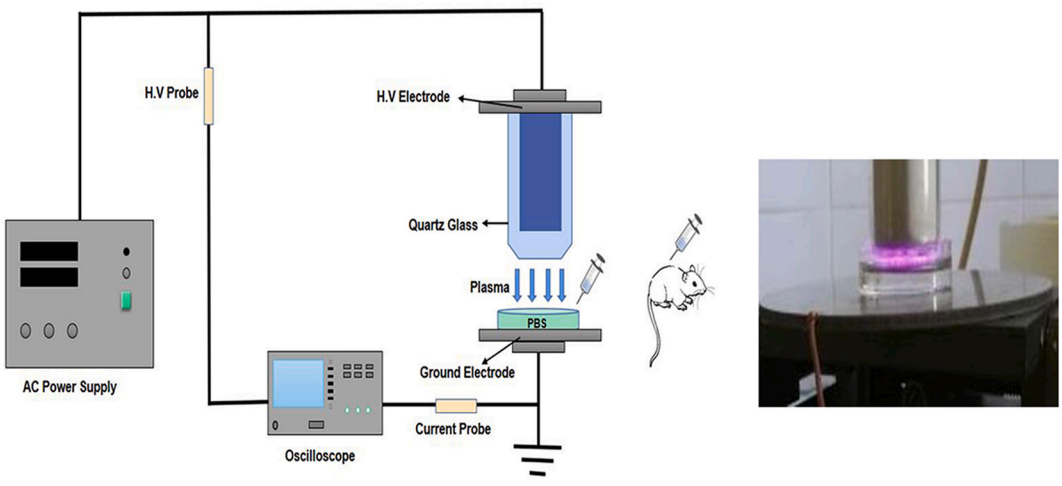

Fig. 1. Diagram of plasma device used in the present study.

developed by the Institute of Plasma Physics, Chinese Academy of Sciences (Fig. 1). The air plasma device was composed of a power source, high-voltage electrode, and ground electrode. A 35-mm cell culture dish with 3 ml PBS was placed between the two electrodes, and the distance from the high-voltage electrode to the liquid surface was 5 mm. After the input voltage and current parameters were adjusted, PAS was prepared by irradiation for different times (1, 3, and 5 min). The plasma discharge voltage and current were monitored by an MSO 5104 digital oscilloscope equipped with a high-voltage probe (P6015A) and a current probe (Tektronix P6021, Tektronix, Bracknell, United Kingdom); the emission spectra were recorded using an AvaSpec 2048 spectrometer (Avantes, Apeldoorn, The Netherlands); and the monitored plasma currents and voltages as well as the emission spectra are shown in Fig. 2A and B.

2.2. Animals and experimental design

Twenty-eight healthy Sprague-Dawley(SD) rats of female between 8 and 12 weeks of age were purchased two weeks before the start of the experiment from Ji'nan Peng Yue Laboratory Animal Breeding Co. Ltd. and had a mean weight of 200 ± 20 g at the beginning of the experiment. These were randomly divided into four groups and kept in cages. The right backs of all animals were shaved after intraperitoneal anesthesia. Animals are kept in identical conditions of temperature and humidity (T: 23 °C, humidity 50 %), with a light and dark cycle of 12 h and were supplied with drinking water and sufficient feed. The experiment was performed on 28 SD rats divided into four groups, with seven in each group. The control group was treated with PBS subcutaneously, and the experimental groups were treated with PAS; 0.3 ml/100 g was used as standard. Injection was done once every 48 h. The rats were euthanized immediately after 10 cycles of therapy. Signs of general toxicity such as changes in the skin, hairiness, diarrhea, >10 % weight loss, behavioral changes, reduced food intake, and depression (decreased motor activity) were observed during treatment. After euthanasia, the treated skin was excised. All animal experiments were conducted according to the guidelines of the Animal Protection and Use Committee of Anhui Medical University and approved by the Animal Experiment Ethics Committee of Anhui Medical University. We focused on reducing animal use and experimental animal pain (approval number: LLSC20221118)

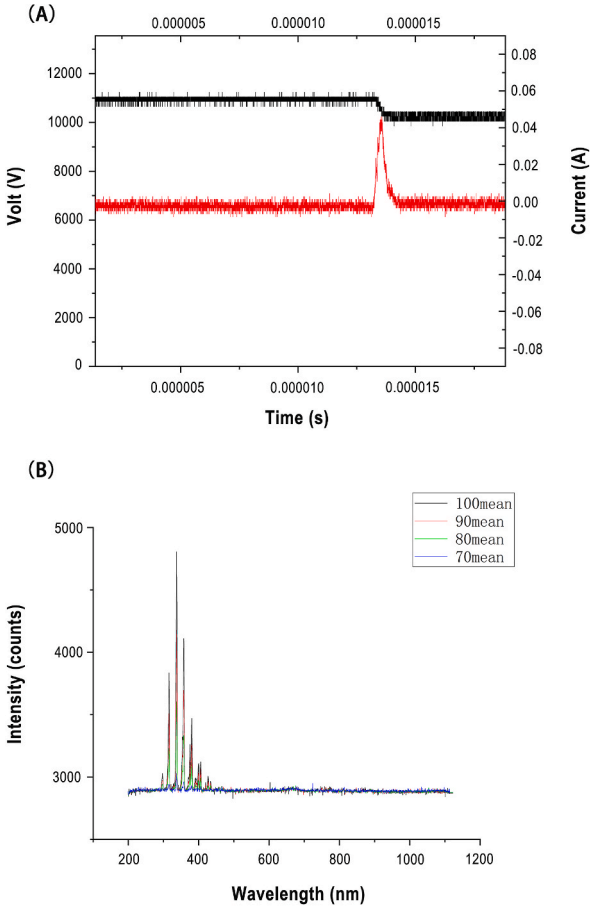

Fig. 2. (A) Current and voltage signal diagram of the plasma center point under specific parameters. (B) Emission spectra of plasma instruments.

2.3. Reactive substance in PAS

It is difficult to establish the rigorous median lethal dose (LD50) or Lethal Concentration 50 (LC50) of PAS at the current stage of this research field, which should be one of the present study limitations. Since our research group found that the time dose had a good anti-tumor cell effect and was selective to normal cells [23], the PAS solution in this study was exposed to plasma for 1, 3, or 5 min H_2O_2 and NO_3^- were measured by the fluorescence microplate reader, along with test kits. The pH changes in different experimental groups were detected using a pH meter.

2.4. Hematology

At the end of the experiment, tissue was harvested by cardiac puncture under isoflurane anesthesia. Blood for hematological studies was collected in sterile negative-pressure anticoagulant tubes and maintained at 20°C–25 °C. To prevent coagulation, we homogenized the blood with anticoagulant in the tube by gently rotating the tube vertically 5–6 times. Hematological assays were performed at the Institute of Pharmacology and Toxicology, Anhui Academy of Medical Sciences. The following parameters were used: white blood cells (WBC), lymphocytes (LYM), monocytes (MON), neutrophils (NEU), red blood cells (RBC), hemoglobin (HGB), mean corpuscular volume (MCV), mean corpuscular hemoglobin (MCH), red cell distribution width (RDWs), red cell distribution width % (RDWc), and platelets (PLT).

2.5. Blood biochemistry

Blood collection for biochemical investigations was performed in 500 μL vacuum tubes with heparin that was kept at room temperature; all the samples were detected and analyzed by Wuhan Servicebio Technology Co., Ltd. The parameters investigated include glutamic pyruvic transaminase (ALT), glutamic oxaloacetic transaminase (AST), blood urea nitrogen (BUN), and creatinine (CREAT).

2.6. Histopathology and immunohistochemistry

After euthanasia with 2 % isoflurane, the weight of individual rat was measured. Tissue samples (myocardium, liver, lungs, and kidneys) were harvested from control and experimental groups, which were washed in normal saline solution, sucked dry with normal filters, weighted, and then fixed in 10 % buffered formalin, and embedded in paraffin. Organ coefficient expressed as the ratio of weight of the organ to animal weight. Since the skin area was directly treated with PAS, it was embedded in paraffin and subjected to trichrome Masson staining (TMS). Phosphorylated histone H2AX (γ-H2AX) was applied for the detection of genomic damage caused by cytotoxic chemical agents, except the histopathological examination for preneoplastic and neoplastic changes of skin epithelium. The detection and visualization of γ-H2AX by immunohistochemistry was used to evaluate DNA damage, related DNA damage proteins, and DNA repair induced by PAS. Ki-67 (a cell proliferation marker) was analyzed by immunohistochemistry to estimate the proliferation grade of epithelial cell populations and improve the diagnostic accuracy of malignant cell proliferation.

The immunohistochemical stain for γ-H2AX was performed using anti-histone H2AX rabbit polyclonal antibody (pAb) from Wuhan Servicebio Technology Co., Ltd. The sections were de-paraffinized, and no retrieval was needed; following an overnight incubation with primary antibodies, the sections were counterstained with Mayer hematoxylin. Finally, samples were dehydrated and mounted for microscopic examination.

Immunohistochemical staining for Ki-67 was performed using a rabbit pAb from Wuhan Servicebio Technology Co., Ltd. The sections were deparaffinized and sequentially treated for antigen epitope retrieval and endogenous peroxidase blocking. After 5 min of infiltration with DAB chromogen solution, the sections were counterstained with Mayer's hematoxylin, dehydrated, and mounted for microscopic examination.

2.7. Superoxide dismutase (SOD) activity and malondialdehyde (MDA) content of the treated skin area

Samples were rinsed with sterile saline (pre-cooled), blood was removed, gently dried, and weighed with a filter paper. After adding sterile saline, the skin was ground using a tissue homogenizer and the final concentration was adjusted to 10 %. Following the instructions of the reagent test kit, the SOD activity and MDA content were determined by Multifunctional enzyme marker.

2.8. Enzyme linked immunosorbent assay

The skin was ground using a tissue homogenizer and centrifuged at 3000 rpm for 10 min to separate the supernatant. The detection of tumor necrosis factor alpha (TNF-α) in the supernatant was performed by ELISA.

2.9. RNA-seq of the treated skin area

After sacrifice, the treated skin area was excised and RNA-seq was performed by Shenzhen Huada Gene Technology Co., Ltd. Sequencing and analysis of differential gene expression were performed by Shenzhen Huada Gene Technology Co., Ltd. The sequencing results were obtained from Shenzhen Huada Gene Technology Co., Ltd. The analysis results report was not shared with a public

database at the time of publication.

2.10. Western blot analysis

Protein samples were separated by sodium dodecyl sulfate-polyacrylamide gel electrophoresis (SDS-PAGE) on 10 % gels and transferred onto polyvinylidene fluoride (PVDF) membranes. The membranes were blocked with 10 % bovine serum (BSA). Subsequently, it was treated with primary antibodies against TGF-β, vascular endothelial growth factor A (VEGFA), and glyceraldehyde-3-phosphate dehydrogenase (GAPDH) overnight at 4 °C. The films were then washed three times with TBST and incubated with goat rabbit anti-IgG or anti-mouse secondary antibodies. After washing the membranes with TBST, a Fino-do X6 analysis system was used to analyze membrane density. ImageJ software was used to quantify the protein bands of interest.

2.11. Statistical analysis

Statistical analyses were performed using IBM SPSS Statistics 25 software (IBM Corp. Armonk, NY, USA). GraphPad Prism (version 7.00; GraphPad Software, Inc.) was used to generate figures. Differences among groups were compared using ANOVA and the Kruskal–Wallis test. The differences between the experimental groups were considered statistically significant at $P < 0.05$.

3. Results

3.1. Active substance in PAS

The pH decreased with the increase of treatment time after plasma treatment, while the concentrations of H_2O_2 and NO_3^- gradually increased compared to the control group. This difference was statistically significant (Fig. 3A–C).

3.2. The organ coefficient and histopathology of vital organs

The organ coefficients were measured after multiple subcutaneous injections of PAS, and there was no significant difference in the organ coefficients between the groups ($P > 0.05$) (Table 1). The results of H&E staining of the organs (heart, lungs, kidneys, and liver) in rats from the four groups are shown in Fig. 4A–D. Compared with the control group, there was no obvious abnormality in the

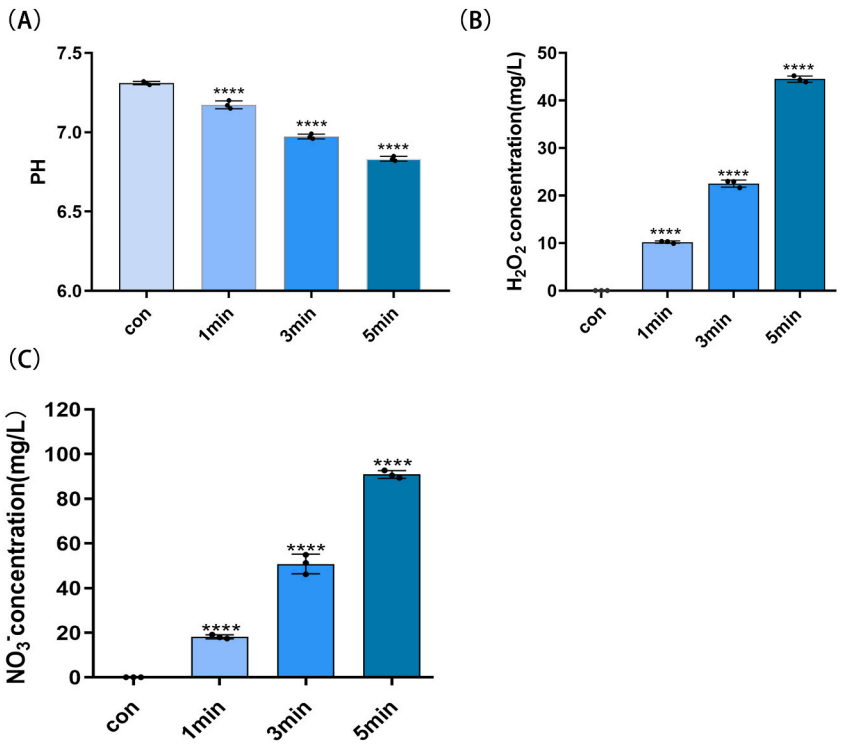

Fig. 3. Detection of changes in reactive species and pH in Plasma-activated solution (PAS). (A): Changes in pH of PAS for different periods. (B): Changes in the H_2O_2 concentration in PAS treated for different periods. (C): Changes in the NO_3 concentration in PAS treated for different periods. $^{****}P < 0.0001$ vs. con.

structure of all levels of bronchial branches and inflammatory changes in the lung. Myocardial fibers were uniformly stained and layered, and no abnormal structural changes were seen in the interstitial tissue. Meanwhile, the liver lobules were clearly demarcated and regularly arranged, and there was no visible inflammatory changes. Finally, the renal corticomedullary border was clear. The glomerulars and tubular epithelial cells were structurally normal, and no obvious inflammatory cell infiltration was observed in the interstitium.

3.3. The effects of blood parameters and biochemical parameters

The mean values of the hematological and biochemical parameters are presented in Table 2. The difference was not statistically significant compared to that in the control group ($P > 0.05$).

3.4. The effect of multiple subcutaneous injections of PAS on healthy skin

Visual inspection of the rat skin did not reveal any damage, such as redness, rash, or skin breakdown. Moreover, no significant histopathological changes or Masson's trichrome staining were observed under the microscope. The epidermis, dermis, and subcutaneous tissue structures of the skin were complete, collagen fibers in the dermis layer were arranged in an orderly manner, and there were no obvious inflammatory cell infiltration and no collagen hyperplasia (Fig. 5A–C).

ROS/RON is the main active substance in PAS. However, excessive content causes redox stress leading to DNA damage and protein and lipid peroxidation, and promotes senescence and even apoptosis of tissue cells [24]. SOD is the most effective antioxidant and free radical scavenger, and its concentration indirectly reflects the ability of body tissues to scavenge free oxygen radicals [25]. MDA, an end product of lipid peroxidation, is an important indicator of the degree of tissue and cell damage caused by free radicals. We measured MAD and SOD in tissues to assess the level of tissue oxidative stress and the severity of lipid peroxidation. SOD and MDA levels in the experimental group did not differ significantly from those in the control group ($P > 0.05$).

The phosphorylated histone H2AX (γ-H2AX) after DNA damage collects at the damage site and directs the DNA repair protein to complete the repair. Thus, the content of γ-H2AX can clearly reflect the degree of DNA damage. We investigated the γ-H2AX content affected by 10 cycles of PAS subcutaneous injections. Immunohistochemical analysis showed no significant difference between the experimental and control group (Fig. 6A and B) ($P > 0.05$).

Ki67, a nuclear antigen associated with cell division, is currently one of the most widely used cell proliferation markers and its expression varies with the cell proliferation cycle [26]. Several studies have reported overexpression of Ki67 in cutaneous squamous cell carcinoma and lung cancer. Immunohistochemical examination of the rat skin that came in direct contact with PAS showed no pre- or neoplastic transformation. There was no expression of Ki-67 proliferation markers in skin cells (Fig. 6C and D).

Tumor necrosis factor-α (TNFα) is a member of the TNF/TNFR cytokine superfamily, and plays a pivotal role in autoimmune and inflammatory diseases and cancer [27]. In mammals, TNFα is a pro-inflammatory cytokine that has a wide range of biological functions. TNF-α affects the growth, differentiation, survival, and physiological function of a variety of different cells, thereby playing an important role in immune response as well as physiological processes such as metabolism and reproduction [28]. Therefore, we were interested in whether the expression of TNF-α is modulated. Consequently, we compared the amount of TNF-α in each group of skin tissue and found no clear difference (shown in Table 2).

3.5. Differentially expressed genes testing with RNA-seq

All DEGs were identified by comparing patients with psoriasis to normal controls. In total, 313 and 227 DEGs were identified, respectively. The results of the expression level analysis of these DEGs are shown in a volcano plot (Fig. 7A and B). Finally, 163 key DEGs were identified by intersection analysis.

To investigate the underlying biological functions of these key DEGs, functional analysis was performed using the DAVID database. The results of GO analysis indicated that transforming growth factor beta receptor signaling pathway, angiogenesis, and negative regulation of gene expression were the top three biological processes (BPs) (Fig. 8A); cytoplasm, perinuclear region of cytoplasm, and cornified envelope were the top three cell components (CCs) (Fig. 8B); mitogen-activated protein kinase binding, SMAD binding, and metallopeptidase activity were the top three molecular functions (MFs) (Fig. 8C). In addition, KEGG pathway analysis revealed that

Table 1
Effect of PAS on organ weight and organ coeffificient[a].

Group	Heart	Liver	Lung	Left kidney	Right kidney
Con	0.004 ± 0.005	0.036 ± 0.005	0.007 (0.0069, 0.0119)	0.003 ± 0.0004	0.004 ± 0.0002
1 min	0.004 ± 0.0003	0.035 ± 0.003	0.009 (0.0074, 0.0106)	0.003 ± 0.0004	0.003 ± 0.0004
3 min	0.004 ± 0.0004	0.035 ± 0.004	0.007 (0.0065, 0.0089)	0.004 ± 0.0008	0.004 ± 0.0005
5 min	0.004 ± 0.0006	0.034 ± 0.003	0.0069 (0.0062, 0.0113)	0.003 ± 0.0005	0.004 ± 0.0003
P value	0.279	0.786	0.703	0.532	0.340

Continuous variables were expressed as the mean ± standard deviation or median (25th, 75th percentile).
PAS: plasma-activated solution.
[a] organ coeffificient was calculated as the ratio of organ weight to body mass.

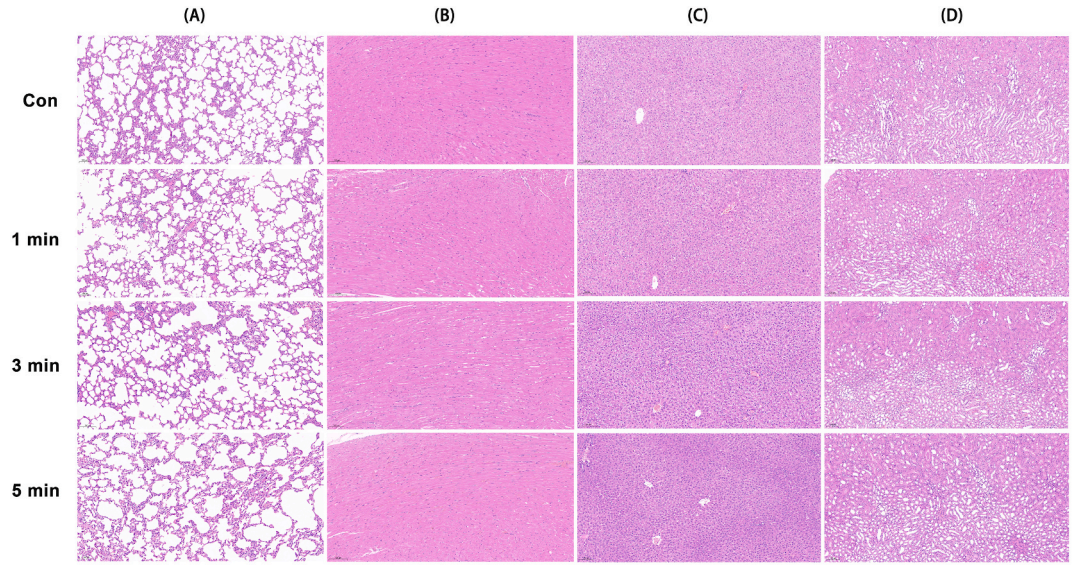

Fig. 4. The histomorphological features of rat organ slices after PAS treatment and in the control (H&E staining, 100× magnification). (A): Lung. (B): Heart. (C): Liver. (D): Kidney.

Table 2
Safety evaluation of PAS injection among three groups and control group.

Parameters	Con	1 min	3 min	5 min
Number of white blood cells (10^9/l)	7.74 ± 3.01	7.75 ± 3.22	4.17 ± 0.79	5.35 ± 0.97
Number of lymphocytes (10^9/l)	5.13 ± 2.24	5.08 ± 2.10	2.48 ± 0.62	3.55 ± 1.08
Number of neutrophils (10^9/l)	1.64 ± 0.50	1.63 ± 0.79	1.02 ± 0.37	1.31 ± 0.33
Number of monocytes (10^9/l)	0.88 ± 0.51	0.89 ± 0.89	0.55 ± 0.31	0.36 ± 0.11
Number of red blood cells (10^{12}/l)	7.58 ± 0.48	7.91 ± 0.82	8.19 ± 0.55	8.84 ± 0.36
Hemoglobin (g l^{-1})	149.75 ± 9.22	153.5 ± 14.36	152.25 ± 6.55	167.25 ± 7.89
mean corpuscular volume (fl)	56.73 ± 1.39	57.5 ± 2.09	54.95 ± 1.53	56.7 ± 1.62
mean corpuscular hemoglobin (pg)	19.78 ± 1.03	19.45 ± 0.87	18.65 ± 0.99	18.93 ± 0.3
Red cell distribution width (%)	12.78 ± 1.05	12.95 ± 1.07	11.98 ± 0.74	13.8 ± 0.91
Platelet count (10^9/l)	949.5 ± 262.21	1014.25 ± 298.52	1104.5 ± 606.13	1084.75 ± 459.59
Alanine transaminase (U/L)[a]	4.14 ± 0.07	3.92 ± 0.08	4.21 ± 0.21	4.16 ± 0.25
Aspartate aminotransferase (U/L)[a]	4.94 ± 0.09	4.56 ± 0.09	4.91 ± 0.28	4.96 ± 0.30
Blood urea nitrogen (mg/dl)	15.99 ± 2.23	17.30 ± 0.38	16.98 ± 1.80	15.89 ± 1.46
Creatinine (umol/L)	40.10 (35.05, 46.56)	44.35(42.95, 46.78)	44.14 (41.61, 45.71)	60.67 (48.61, 77.99)
Superoxide dismutase (U/mg)[a]	2.69 ± 0.19	3.03 ± 0.20	2.89 ± 0.29	3.01 ± 0.25
Malondialdehyde (nmol/mg)[a]	0.06 ± 0.02	0.07 ± 0.03	0.07 ± 0.03	0.08 ± 0.03
Tumor necrosis factor-α (pg/ml)	−0.05 ± 0.48	0.28 ± 0.29	0.11 ± 0.24	−0.23 ± 0.39

Continuous variables were expressed as the mean ± standard deviation or median (25th, 75th percentile).
PAS: plasma-activated solution.
a These data were transformed into logarithms to improve the skewed distribution.

key DEGs were significantly enriched in proteoglycans in cancer, tight junctions, and the AGE-RAGE signaling pathway in diabetic complications (Fig. 8D).

Subsequently, we measured the expression of TGF-β and VEGFA after local injection of PAS. Compared with the control group, the expression activity of TGF-β and VEGFA after subcutaneous injection of PAS was increased, however, there was no significant difference between PAS 1 min, PAS 3 min, and PAS 5 min (Fig. 9A and B).

4. Discussion

PAS as a "drug"has received widespread attention for sterilization and anti-tumor research. It can be stored at room temperature and allows easy transportation while retaining anticancer and antiseptic properties [29]. However, there is no unified and standardized management standard for setting the CAP equipment working parameters and safety evaluation [30,31]. Our group has previously shown that PAS can inhibit the proliferation of isolated skin basal cell carcinoma and squamous cell carcinoma in a dose-dependent and time-dependent manner, and has obvious selectivity for HaCaT keratinocytes, as well as obvious bacteriostatic effects [6,23]. Whether PAS affects normal skin tissue cells when injected subcutaneously to treat benign and malignant tumors such as

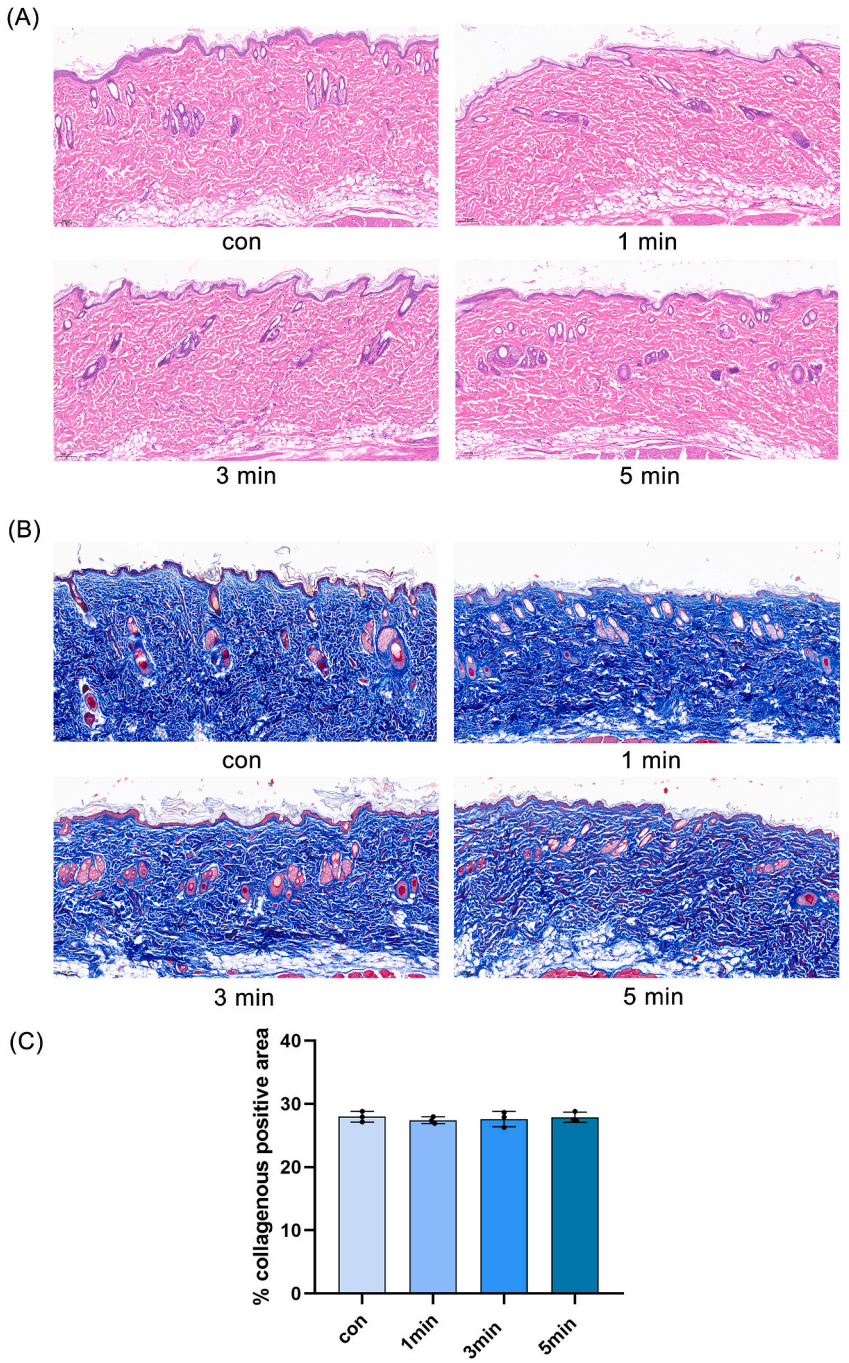

Fig. 5. Microscopic view of rat skin tissue after PAS treatment and in the control. (A): H&E staining, 100× magnification. (B): Masson's trichrome staining, 100× magnification. (C) Semiquantitative analysis of collagenous fiber positive area.

basal cell carcinoma, squamous cell carcinoma, malignant melanoma, hemangioma, and infections of the skin is currently unknown. In this study, the effect of multiple subcutaneous injections of PAS on normal skin tissue and vital organs was detected, which showed that the local injection site of PAS promoted the overexpression of TGF-β and VEGFA without the proliferation, migration, or death of keratinocytes, fibroblasts, and the increase of collagen fibers. Moreover, the solution was not toxic to the heart, lungs, liver, kidneys, or other major organs.

It is difficult to detect the content of short-lived active substances in PAS because of their short reactivities and half-cycles [23]. We measured the pH of PAS and the concentrations of the main longevity active components H_2O_2 and NO_3^- (RNS), and found that with the prolongation of violent times, pH decreased and levels of H_2O_2 and NO_3^- increased. ROS and RNS exert important biological roles in

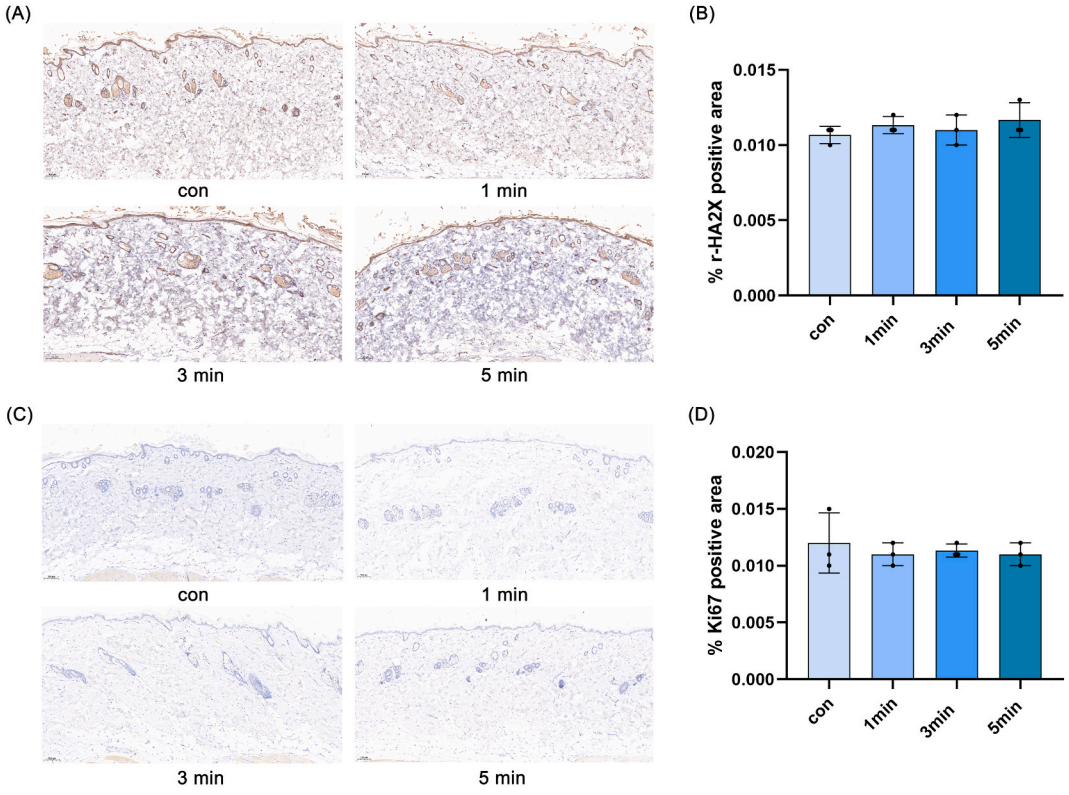

Fig. 6. Immunohistochemistry—signals of γ-H2AX and Ki-67 markers of rat skin tissue in the different groups. (A): γ-H2AX. (B) Semiquantitative analysis of γ-H2AX positive area. (C): Ki-67. (D) Semiquantitative analysis of Ki-67 positive area.

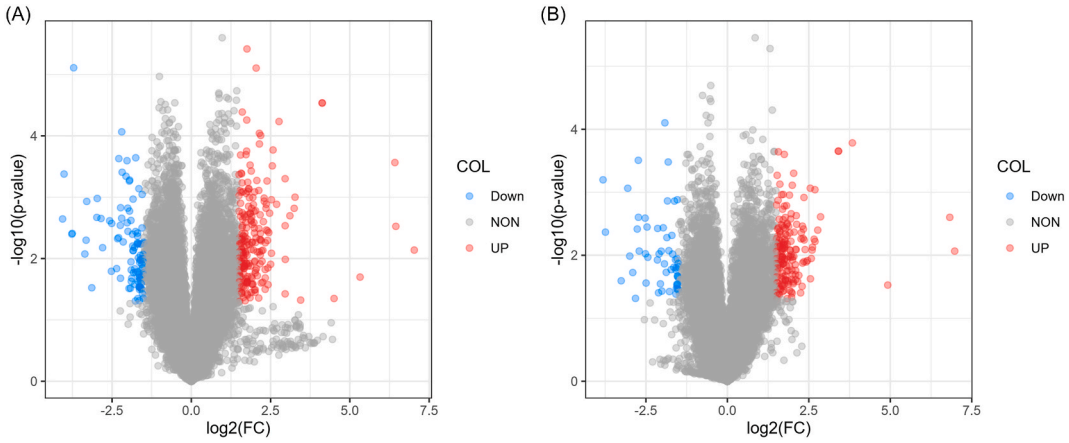

Fig. 7. Representation of differential expressed genes in form of Volcano plot with red dots showing upregulated genes while blue dots showing downregulated genes. (A): Plasma-activated solution:1 min vs con. (B): plasma-activated solution: 5 min vs con.

cellular function, but excess ROS/RON may have toxic effects on cells [20,21]. The cell selectivity of PAS was also evaluated by in vitro experiments on the effect of PAS on the viability of Hacat, malignant melanoma, and squamous cell carcinoma cells. It was found that PAS showed good biocompatibility, and the cell viability of Hacat cells was much higher than that of tumor cells [32]. Nakamura K et al. reported the inhibitory effect of plasma-activated medium (PAM) on the metastasis of ovarian cancer ES2 cells in vitro and in vivo. Meanwhile, In an in vivo mouse model of intraperitoneal metastasis, PAM inhibited peritoneal dissemination of ES2 cells, resulting in prolonged survival [33].

Emerging evidence has shown that PAS is not toxic to vital organs in animals with immunodeficiency, wounds, or tumors [34–36]. However, studies using multiple subcutaneous treatments for PAS have not been reported. In this study, we evaluated the differences in

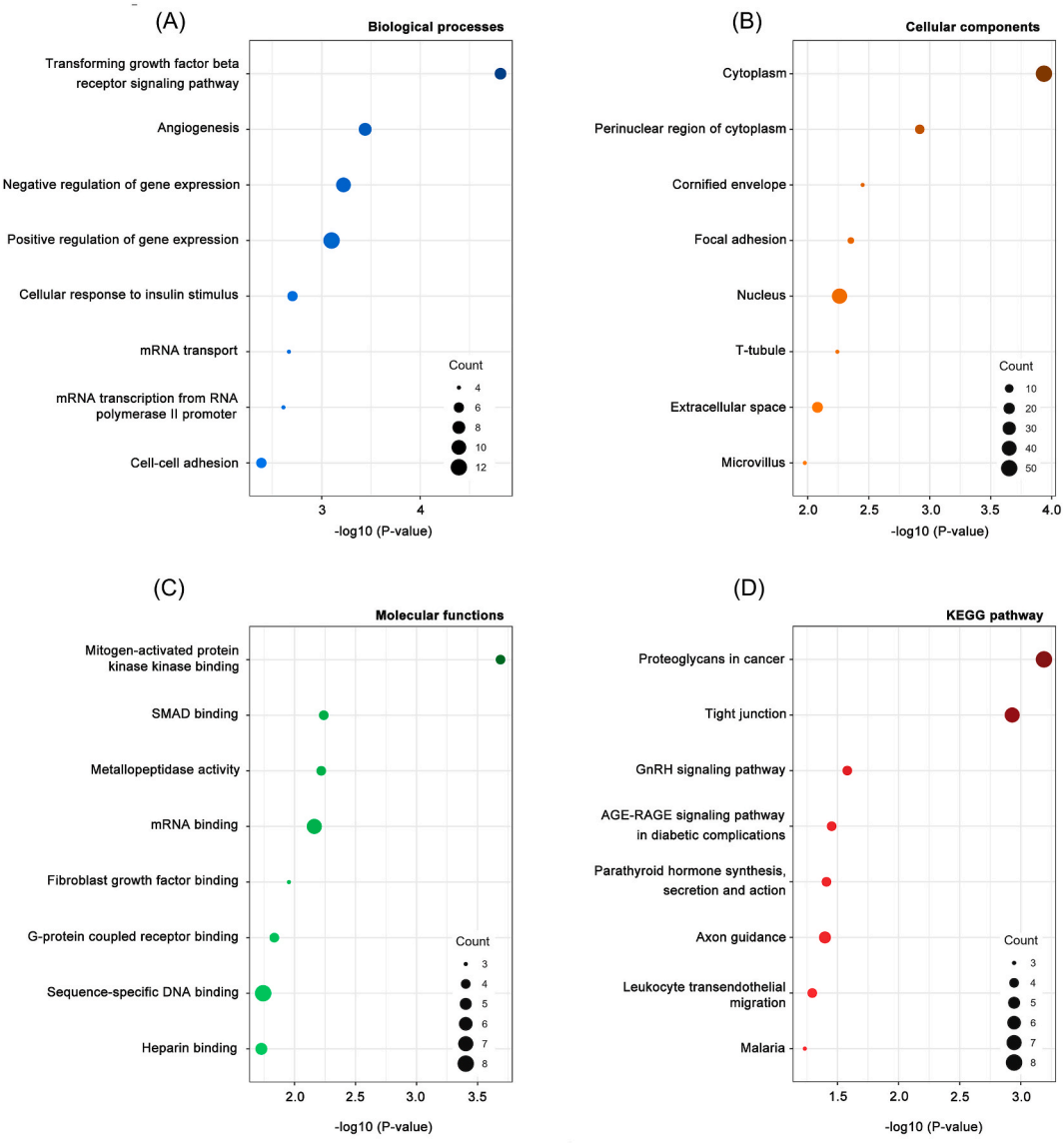

Fig. 8. GO and KEGG pathway enrichment analysis of DEGs. (A): Gene ontology in terms of Biological processes. (B): Gene ontology in terms of Cellular Components. (C): Gene ontology in terms of Molecular function. (D): KEGG pathway analysis.

macroscopic organ coefficient, histopathological examination, hematology, and blood biochemistry indicators of vital organs (heart, lung, kidney, and liver) and confirmed that multiple subcutaneous injections of PAS had no significant negative effect on some vital organs.

Most studies have indicated that apoptotic mechanisms induced by PAS include oxidative stress, DNA damage [37,38], and mitochondrial dysfunction [38–40]. The ROS/RON of PAS induce lipid peroxidation of the bacterial wall and affect intracellular components to generate effects of sterilization and disinfection [40,41]. However, oxidative stress in cancer cells induced by ROS is critical for the selective treatment of cancer cells, as it is the reserved antioxidant of normal cells that prevents cellular ROS levels from reaching the fatal threshold [36]. intracellular ROS levels increase due to metabolic abnormalities and oncogenic signaling in cancer cells. Therefore, when both normal cells and cancer cells are exposed to a given amount of exogenous ROS stress, the intracellular ROS levels in cancer cells reach the toxicity threshold more easily than in normal cells [36]. However, if the amount of ROS in normal cells is high enough that the threshold is exceeded, redox homeostasis is disrupted, which leads to oxidative damage to lipids, proteins, and DNA, and toxic cellular effects [38,39]. In this study, the oxidative balance of local tissues after PAS injection was evaluated by detecting SOD and MAD levels in skin tissues, thereby showing that there were no significant differences among the groups. Meanwhile, we assessed the extent of DNA damage by detecting the concentration of γ-H2AX, which reflected that DNA damage was not caused after PAS injection. This indicates that the oxidation and antioxidant capacity of normal skin tissue cells were in a relatively balanced state.

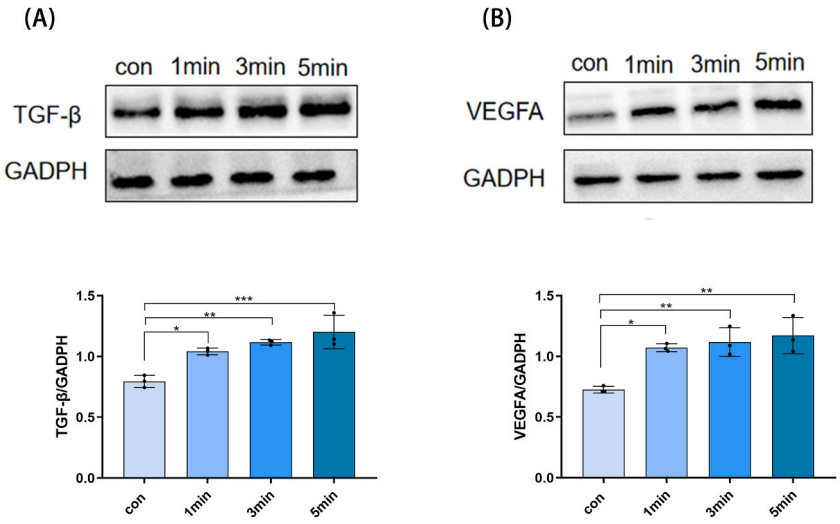

Fig. 9. After subcutaneous of PBS and the plasma-activated solution, the expression of TGF-β and VEGFA is analyzed by western blotting. (A): Immunoblots and representative graphs showing the protein expression of TGF-β. (B): Immunoblots and representative graphs showing the protein expression of VEGFA. $^{*}P < 0.05, ^{**}P < 0.01, ^{***}P < 0.001$ vs. con.

TGF-β and VEGF are secreted from the epidermis and dermis, which is known to play a significant role in anti-aging and tissue regeneration. Direct effects of plasma on skin activation was investigated by Choi et al. who found that CAP treatment on skin induced the expression of TGF-β and VEGF without causing any damage [42]. Inconsistent with other studies, this study focused on the direct subcutaneous injection of PAS. Meanwhile, ROS/RON were in more direct contact with normal skin tissue, which makes it easier to manifest their effects on molecular changes in skin tissue and potential toxicity. DEGs in tissues after subcutaneous injection of PAS were identified using RNA-seq. Compared with the control group, the TGF-β receptor signaling pathway and biological process of angiogenesis were significantly upregulated. Subsequently, an increase in TGF-β, VEGFA expression was detected by Western blot. In addition, no abnormal structural changes, including pathological collagen deposition, angiogenesis and inflammatory changes, were seen in the histopathological tests, which indicates that the low-temperature plasma activation solution does not produce pathological damage when it is applied subcutaneously to the skin tissue.

5. Conclusions

In our study, the body weight and behavior of the rats were not abnormal after 10 injections of PAS, and there were also no adverse effects on the structure and homeostasis of the major organs. The local injection site did not show redness, swelling, or ruptured rashes. Histological evidence showed that PAS had no effect on the proliferation of keratinocytes and fibroblasts, and did not cause an increase in collagen fibers. These results indicate that multiple subcutaneous injections of PAS did not show significant toxic effects on local skin tissues and some major organs in rats. However, this finding needs to be further confirmed in future clinical studies.

Declarations

All animal experiments were conducted according to the guidelines of the Animal Protection and Use Committee of Anhui Medical University and approved by the Animal Experiment Ethics Committee of Anhui Medical University. We focused on reducing animal use and experimental animal pain (approval number: LLSC20221118).

Data availability statement

The data of this study are available on reasonable request from the corresponding author.

CRediT authorship contribution statement

Fanfan Chen: Writing – review & editing, Writing – original draft, Methodology, Investigation, Formal analysis, Conceptualization. **Houyu He:** Writing – review & editing, Writing – original draft, Methodology, Investigation, Formal analysis, Conceptualization. **Liyun Wang:** Resources, Project administration, Methodology, Investigation. **Xingyu Yang:** Investigation. **Jing Gao:** Resources, Project administration, Methodology, Investigation. **Jingwen Wang:** Resources, Project administration, Methodology, Investigation. **Shengquan Zhang:** Investigation. **Shenghai Huang:** Investigation. **Chunjun Yang:** Writing – review & editing, Writing – original draft, Visualization, Validation, Supervision, Funding acquisition, Conceptualization.

Declaration of competing interest

The authors declare that they have no known competing financial interests or personal relationships that could have appeared to influence the work reported in this paper.

Acknowledgments

This work was supported by Natural Science Research Project of Anhui Colleges and Universities, China [KJ2020ZD19]; Clinical Training Program of the Second Affiliated Hospital of Anhui Medical University, China [2020LCZD21]; Anhui Provincial People's Government modern medical and pharmaceutical industry development several policy support projects; Basic and Clinical Cooperative Research Promotion Program of Anhui Medical University, China [2020XKJT042]; Incubation Program of National Natural Science Foundation of China, The Second Affiliated Hospital of Anhui Medical University, China [2021GQFY03]; Research Fund of Anhui Institute of Translational Medicine, China [2021ZHYX-C48]; Clinical Medicine Discipline Construction Project of Anhui Medical University, China, and Scientific research fund project of Anhui Medical University, China [2022XKJ048].

Appendix A. Supplementary data

Supplementary data to this article can be found online at https://doi.org/10.1016/j.heliyon.2023.e23116.

References

[1] M. Laroussi, Nonthermal decontamination of biological media by atmospheric-pressure plasmas: review, analysis, and prospects, IEEE Trans. Plasma Sci. Soc. 30 (4) (2002) 1409–1415.
[2] P. Awakowicz, N. Bibinov, M. Born, B. Busse, R. Gesche, A. Helmke, A. Kaemling, V. Kolb Bachofen, R. Kovacs, S. Kuehn, Biological stimulation of the human skin applying healthpromoting light and plasma sources, Contrib. Plasma Phys. 49 (9) (2009) 641–647.
[3] J. Heinlin, G. Morfill, M. Landthaler, W. Stolz, G. Isbary, J.L. Zimmermann, T. Shimizu, S. Karrer, Plasma medicine: possible applications in dermatology, J. Dtsch. Dermatol. Ges. 8 (12) (2010) 968–976.
[4] E. Robert, T. Darny, S. Dozias, S. Iseni, J.M. Pouvesle, New insights on the propagation of pulsed atmospheric plasma streams: from single jet to multi jet arrays, Phys. Plasmas 22 (12) (2015).
[5] A. Bourdon, T. Darny, F. Pechereau, J.M. Pouvesle, P. Viegas, S. Iséni, E. Robert, Numerical and experimental study of the dynamics of a μs helium plasma gun discharge with various amounts of N2 admixture, Plasma Sources Sci. Technol. 25 (3) (2016).
[6] J. Liu, C. Yang, C. Cheng, C. Zhang, J. Zhao, C. Fu, In vitro antimicrobial effect and mechanism of action of plasma-activated liquid on planktonic Neisseria gonorrhoeae, Bioengineered 12 (1) (2021) 4605–4619.
[7] H. Tanaka, K. Ishikawa, M. Mizuno, S. Toyokuni, H. Kajiyama, F. Kikkawa, H. Metelmann, M. Hori, State of the art in medical applications using non-thermal atmospheric pressure plasma, Rev. Mod. Plasma Phys. 1 (1) (2017) 1–89.
[8] K. Miyamoto, S. Ikehara, H. Takei, Y. Akimoto, H. Sakakita, K. Ishikawa, M. Ueda, J. Ikeda, M. Yamagishi, J. Kim, Red blood cell coagulation induced by low-temperature plasma treatment, Arch. Biochem. Biophys. 605 (2016) 95–101.
[9] H. Tanaka, M. Mizuno, K. Ishikawa, S. Toyokuni, H. Kajiyama, F. Kikkawa, M. Hori, Molecular mechanisms of non-thermal plasma-induced effects in cancer cells, Biol. Chem. 400 (1) (2019) 87–91.
[10] H. Tanaka, M. Mizuno, K. Ishikawa, S. Toyokuni, H. Kajiyama, F. Kikkawa, M. Hori, New hopes for plasma-based cancer treatment, Plasma 1 (1) (2018) 150–155.
[11] C. Weishaupt, S. Emmert, Connecting basic cold plasma technology to dermato-oncology, Clin. Plasma Med. 10 (2018) 16–19.
[12] A. Privat-Maldonado, A. Schmidt, A. Lin, K. Weltmann, K. Wende, A. Bogaerts, S. Bekeschus, ROS from physical plasmas: redox chemistry for biomedical therapy, Oxid. Med. Cell. Longev. 2019 (2019), 9062098.
[13] G. Busco, E. Robert, N. Chettouh-Hammas, J.M. Pouvesle, C. Grillon, The emerging potential of cold atmospheric plasma in skin biology, Free Radic. Biol. Med. 161 (2020) 290–304.
[14] G. Fridman, G. Friedman, A. Gutsol, A.B. Shekhter, V.N. Vasilets, A. Fridman, Applied plasma medicine, Plasma Process. Polym. 5 (6) (2008) 503–533.
[15] D. Xu, S. Wang, B. Li, M. Qi, R. Feng, Q. Li, H. Zhang, H. Chen, M.G. Kong, Effects of plasma-activated water on skin wound healing in mice, Microorganisms 8 (7) (2020) 1091.
[16] V. Vijayarangan, A. Delalande, S. Dozias, J.M. Pouvesle, E. Robert, C. Pichon, New insights on molecular internalization and drug delivery following plasma jet exposures, Int. J. Pharm. 589 (2020).
[17] V. Vijayarangan, S. Dozias, C. Heusele, O. Jeanneton, C. Nizard, C. Pichon, J.M. Pouvesle, A. Stancampiano, E. Robert, Boost of cosmetic active ingredient penetration triggered and controlled by the delivery of kHz plasma jet on human skin explants, Front. Physiol. 11 (2023).
[18] J. Balzer, K. Heuer, E. Demir, M.A. Hoffmanns, S. Baldus, P.C. Fuchs, P. Awakowicz, C.V. Suschek, C. Opländer, Non-thermal dielectric barrier discharge (DBD) effects on proliferation and differentiation of human fibroblasts are primary mediated by hydrogen peroxide, PLoS One 10 (12) (2015), e144968.
[19] A. Schmidt, S. Dietrich, A. Steuer, K. Weltmann, T. von Woedtke, K. Masur, K. Wende, Non-thermal plasma activates human keratinocytes by stimulation of antioxidant and phase II pathways, J. Biol. Chem. 290 (11) (2015) 6731–6750.
[20] G.J. Kim, W. Kim, K.T. Kim, J.K. Lee, DNA damage and mitochondria dysfunction in cell apoptosis induced by nonthermal air plasma, Appl. Phys. Lett. 96 (2) (2010).
[21] M.Y. Alkawareek, N.H. Alshraiedeh, S. Higginbotham, P.B. Flynn, B.F. Gilmore, Plasmid DNA damage following exposure to atmospheric pressure nonthermal plasma: kinetics and influence of oxygen admixture, Plasma Med. 4 (1–4) (2015) 211–219.
[22] X.P. Lu, P.J. Bruggeman, S. Reuter, G. Naidis, A. Bogaerts, M. Laroussi, M. Keidar, E. Robert, J.M. Pouvesle, D.W. Liu, K. Ostrikov, Grand challenges in low temperature plasmas, Front. Physiol. 10 (2022).
[23] X. Yang, C. Yang, L. Wang, Z. Cao, Y. Wang, C. Cheng, G. Zhao, Y. Zhao, Inhibition of basal cell carcinoma cells by cold atmospheric plasmaactivated solution and differential gene expression analysis, Int. J. Oncol. 56 (5) (2020) 1262–1273.
[24] N. Yoshikawa, K. Nakamura, H. Kajiyama, Current understanding of plasma-activated solutions for potential cancer therapy, Free Radic. Res. 57 (2) (2023) 69–80.
[25] O.M. Ighodaro, O.A. Akinloye, First line defence antioxidants-superoxide dismutase (SOD), catalase (CAT) and glutathione peroxidase (GPX): their fundamental role in the entire antioxidant defence grid, Alex. J. Med. 54 (4) (2018) 287–293.
[26] T. Scholzen, J. Gerdes, The Ki-67 protein: from the known and the unknown, J. Cell. Physiol. 182 (3) (2000) 311–322.

[27] B.B. Aggarwal, S.C. Gupta, J.H. Kim, Historical perspectives on tumor necrosis factor and its superfamily: 25 years later, a golden journey, Blood 119 (3) (2012) 651–665.
[28] F.W. Goetz, J.V. Planas, S. MacKenzie, Tumor necrosis factors, Dev. Comp. Immunol. 28 (5) (2004) 487–497.
[29] L. Gao, X. Shi, X. Wu, Applications and challenges of low temperature plasma in pharmaceutical field, J. Pharm. Anal. 11 (1) (2021) 28–36.
[30] K. Wende, S. Straßenburg, B. Haertel, M. Harms, S. Holtz, A. Barton, K. Masur, T. von Woedtke, U. Lindequist, Atmospheric pressure plasma jet treatment evokes transient oxidative stress in HaCaT keratinocytes and influences cell physiology, Cell Biol. Int. 38 (4) (2014) 412–425.
[31] K.P. Arjunan, V.K. Sharma, S. Ptasinska, Effects of atmospheric pressure plasmas on isolated and cellular DNA—a review, Int. J. Mol. Sci. 16 (2) (2015) 2971–3016.
[32] H. Motaln, N. Recek, B. Rogelj, Intracellular responses triggered by cold atmospheric plasma and plasma-activated media in cancer cells, molecules 26 (5) (2021) 1336.
[33] K. Nakamura, Y. Peng, F. Utsumi, H. Tanaka, M. Mizuno, S. Toyokuni, M. Hori, F. Kikkawa, H. Kajiyama, Novel intraperitoneal treatment with non-thermal plasma-activated medium inhibits metastatic potential of ovarian cancer cells, Sci. Rep. 7 (1) (2017) 6085.
[34] H. Zhang, S. Xu, J. Zhang, Z. Wang, D. Liu, L. Guo, C. Cheng, Y. Cheng, D. Xu, M.G. Kong, Plasma-activated thermosensitive biogel as an exogenous ROS carrier for post-surgical treatment of cancer, Biomaterials 276 (2021), 121057.
[35] F. Ye, H. Kaneko, Y. Nagasaka, R. Ijima, K. Nakamura, M. Nagaya, K. Takayama, H. Kajiyama, T. Senga, H. Tanaka, Plasma-activated medium suppresses choroidal neovascularization in mice: a new therapeutic concept for age-related macular degeneration, Sci. Rep. 5 (1) (2015) 1–7.
[36] J.M. Joslin, J.R. McCall, J.P. Bzdek, D.C. Johnson, B.M. Hybertson, Aqueous plasma pharmacy: preparation methods, chemistry, and therapeutic applications, Plasma Med. 6 (2) (2016) 135–177.
[37] S. Arndt, E. Wacker, Y.F. Li, T. Shimizu, H.M. Thomas, G.E. Morfill, S. Karrer, J.L. Zimmermann, A.K. Bosserhoff, Cold atmospheric plasma, a new strategy to induce senescence in melanoma cells, Exp. Dermatol. 22 (4) (2013) 284–289.
[38] S.U. Kang, J.H. Cho, J.W. Chang, Y.S. Shin, K.I. Kim, J.K. Park, S.S. Yang, J.S. Lee, E. Moon, K. Lee, Nonthermal plasma induces head and neck cancer cell death: the potential involvement of mitogen-activated protein kinase-dependent mitochondrial reactive oxygen species, Cell Death Dis. 5 (2) (2014), e1056.
[39] G.J. Kim, W. Kim, K.T. Kim, J.K. Lee, DNA damage and mitochondria dysfunction in cell apoptosis induced by nonthermal air plasma, Appl. Phys. Lett. 96 (2) (2010), 21502.
[40] L. Su, J. Zhang, H. Gomez, R. Murugan, X. Hong, D. Xu, F. Jiang, Z. Peng, Reactive oxygen species-induced lipid peroxidation in apoptosis, autophagy, and ferroptosis, Oxid. Med. Cell. Longev. 2019 (2019), 5080843.
[41] D. Del Rio, A.J. Stewart, N. Pellegrini, A review of recent studies on malondialdehyde as toxic molecule and biological marker of oxidative stress, Nutr. Metabol. Cardiovasc. Dis. 15 (4) (2005) 316–328.
[42] B. Choi, J.H. Choi, J. Ji, K.W. Song, H.J. Lee, G.C. Kim, Increment of growth factors in mouse skin treated with non-thermal plasma, Int. J. Med. Sci. 15 (11) (2018) 1203–1209.